International Journal of Engineering, Mathematical and Physical Sciences
ISSN: 2517-9934
Vol:6, No:6, 2012

Numerical Simulation of unsteady MHD Flow and Heat Transfer of a Second Grade Fluid with Viscous Dissipation and Joule Heating using Meshfree Approach

R. Bhargava, Sonam Singh

Abstract**—**In the present study, a numerical analysis is carried out to investigate unsteady MHD (magneto-hydrodynamic) flow and heat transfer of a non-Newtonian ***second grade viscoelastic fluid*** over an ***oscillatory stretching sheet***. The flow is induced due to an infinite elastic sheet which is stretched oscillatory (back and forth) in its own plane. Effect of viscous dissipation and joule heating are taken into account. The non-linear differential equations governing the problem are transformed into system of non-dimensional differential equations using similarity transformations. A newly developed ***meshfree*** numerical technique ***Element free Galerkin method (EFGM)*** is employed to solve the coupled non linear differential equations. The results illustrating the effect of various parameters like viscoelastic parameter, Hartman number, relative frequency amplitude of the oscillatory sheet to the stretching rate and Eckert number on velocity and temperature field are reported in terms of graphs and tables. The present model finds its application in polymer extrusion, drawing of plastic films and wires, glass, fiber and paper production etc.

Keywords**—**EFGM, MHD, Oscillatory stretching sheet, Unsteady, Viscoelastic

I. Introduction

In many fluids such as blood, dyes, yoghurt, ketchup, shampoo, mud, clay etc. the relation between stress and strain can't be simply described by Newton's law of viscosity and are usually called non-Newtonian fluids. The flows of such type of fluids have immense practical applications in polymer devolatisation, fermentation, plastic foam processing and many others. To study the behavior of non-Newtonian fluids, various models have been proposed by many authors taking account of variations of their rheological properties. One of the most popular models for non-Newtonian fluids is the model of second order fluids which is given by

$$T = -pI + \mu A_1 + \alpha_1 A_2 + \alpha_2 A_1^2 \qquad (1)$$

Where T is the Cauchy stress tensor, p is the pressure, α_1 *and* α_2 are material constants, and A_1, A_2 are defined as,

$$A_1 = (grad\, V) + (grad\, V)^T$$

$$A_2 = \frac{d}{dt} A_1 + A_1.(grad\, V) + (grad\, V)^T .A$$

The sign of the material constants α_1 and α_2 is the subject of much controversy which was discussed by Dunn and Rajagopal [1]. Generally, in the literature the fluid which satisfies (1) with $\mu > 0, \alpha_1 > 0, \alpha_1 + \alpha_2 = 0$ is known as second grade fluid while fluid with restriction $\mu > 0, \alpha_1 < 0, \alpha_1 + \alpha_2 \neq 0$ is termed as second order fluid. When $\mu > 0, \alpha_1 = \alpha_2 = 0$,(1) reduces to the well-known constitutive relation of an incompressible Newtonian fluid.

The problems of flow and heat transfer due to a continuously moving stretching surface through an ambient fluid have received much attention in past. Such problems find their application over a broad spectrum of science and engineering disciplines, eg. aerodynamic extrusion of plastic sheets, the cooling of an infinite metallic plate in a cooling bath, the boundary layer along a liquid film in condensation process, and paper production. The dynamics of boundary layer flow over a moving continuous solid surface was originated from the pioneer work of Sakiadis [2]. Then, Crane [3] initiated the analytical study of boundary layer flow of a Newtonian fluid over a linearly stretching surface. Due to recent advances in no-Newtonian fluids, it is still of interest to simulate stretching flows involving non-Newtonian fluids. Wang [4] discussed the viscous flow due to an oscillatory stretching surface. Ambethkar [5] discussed the oscillatory motion of a viscoelastic fluid past a stretching sheet with thermal relaxation. In the present study we provide an attempt for the numerical simulation of moment and heat transfer of a second grade viscoelastic fluid over an oscillatory stretching sheet. Although flow is induced by oscillatory stretching sheet in the present analysis but we also have a free stream velocity oscillating in time about a constant mean oscillatory flow [6]-[7]. The non-linear mathematical model of the problem is solved by a meshless numerical technique known as Element free Galerkin method which is a very powerful technique and has been successfully employed to solve various problems in different areas such as heat transfer [8], fracture mechanics [9] etc. Recently, Singh and Bhargava [10] have applied EFGM for the simulation of an unsteady micropolar squeeze film flow. Results obtained with EFGM are compared with some results reported by Chen [11] and Grubka and Bobba [12] in table I and excellent agreement has been observed between them.

R. Bhargava is a professor at department of mathematics, I.I.T. Roorkee, India. (phone: +919319650553; e-mail: rbharfma@iitr.ernet.in).

Sonam Singh is a research scholar at department of mathematics, I.I.T. Roorkee, India. (phone: +919761076389; e-mail: sonamdma@iitr.ernet.in).

II. Mathematical Analysis

Consider the two-dimensional unsteady MHD flow of an incompressible viscoelastic fluid (obeying second grade model) in the presence of viscous dissipation and joule heating past an oscillatory stretching surface coinciding with the plane $y = 0$ and the flow being confined to the space $y > 0$.

The flow is generated by stretching of an elastic boundary sheet which is stretched back and forth periodically with velocity $u_w = bx \sin \omega t$ parallel to x axis, where b is the stretching rate and ω is the oscillation frequency of the sheet. x- and y-axis are taken as the coordinates along the sheet and normal to it respectively. Further u and v are the velocity components along the x- and y-directions respectively. The fluid moves in the x-direction with a velocity (u-component) equal to the velocity of the solid surface, whereas at increasing distance from the surface, the velocity of the fluid approaches to zero asymptotically. The physical model and geometrical coordinates are shown in Fig. 1.

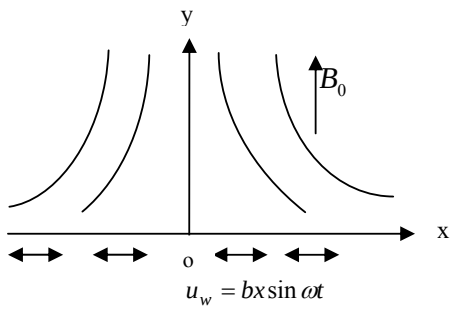

Fig. 1 Geometry of the problem

A constant magnetic field of strength B_0 is applied perpendicular to the stretching surface and the effect of the induced magnetic field is neglected. All the fluid properties are assumed to be isotropic and constant. With the usual boundary layer approximation, the governing equations for unsteady magneto-hydrodynamic momentum and heat transfer for a second grade viscoelastic fluid in the presence of viscous dissipation and joule heating take the following from:

$$\frac{\partial u}{\partial x} + \frac{\partial v}{\partial y} = 0 \tag{2}$$

$$\frac{\partial u}{\partial t} + u\frac{\partial u}{\partial x} + v\frac{\partial u}{\partial y} = \nu\frac{\partial^2 u}{\partial y^2} + k_0\left(\frac{\partial^3 u}{\partial t \partial y^2} + \frac{\partial}{\partial x}\left(u\frac{\partial^2 u}{\partial y^2}\right) + v\frac{\partial^3 u}{\partial y^3} + \frac{\partial u}{\partial y}\frac{\partial^2 v}{\partial y^2}\right) - \frac{\sigma B_0^2}{\rho}u \tag{3}$$

$$\rho c_p\left(\frac{\partial T}{\partial t} + u\frac{\partial T}{\partial x} + v\frac{\partial T}{\partial y}\right) = K\frac{\partial^2 T}{\partial y^2} + \mu\left(\frac{\partial u}{\partial y}\right)^2 + \sigma B_0^2 u^2 \tag{4}$$

Where μ, ν are the dynamic and kinematic viscosity of the fluid, ρ is the fluid density, σ is the electrical conductivity of the fluid, k_0 is the viscoelastic parameter of the fluid, K is the thermal conductivity of the fluid and c_p is the specific heat at constant pressure.

The following appropriate boundary conditions are employed on the velocity field:

$$u = u_w = bx \sin \omega t, \quad v = 0 \; at \; y = 0, t > 0 \tag{5}$$

$$u = 0, \frac{\partial u}{\partial y} = 0 \quad as \; y \to \infty \tag{6}$$

An augmented boundary condition for longitudinal velocity gradient has been used in (6) following Fosdick and Rajagopal [13]. Physical implication of this boundary condition is the absence of shear stress in free stream. Since (3) is a third order differential equation in u whereas without the augmented boundary condition the prescribed boundary conditions on u are two. Hence, without the augmented boundary condition in (6) above system is ill-posed. In (5), both ω and b have the dimension (time)$^{-1}$. We assume, $S = \frac{\omega}{b}$ which denotes the ratio of oscillation frequency of the sheet to its stretching rate.

The boundary conditions for the temperature field are given as follows:

$$T = T_w = T_\infty + A\left(\frac{x}{l}\right)^2 \quad at \; y = 0 \tag{7}$$

$$T \to T_\infty \quad as \; y \to \infty \tag{8}$$

Where A is a constant and l is the characteristic length.

III. Transformation of the Model

To examine the flow regime adjacent to the sheet the following transformations are invoked,

$$\eta = \sqrt{\frac{b}{\nu}}y, \quad \tau = t\omega$$

$$u = bx f_\eta(\eta, \tau), \quad v = -\sqrt{\nu b}\, f(\eta, \tau), \quad \theta(\eta, \tau) = \frac{T - T_\infty}{T_W - T_\infty} \tag{9}$$

Using transformations (9), the continuity equation is automatically satisfied and the governing equations (3), (4) are reduced to following non-dimensional form,

$$S f_{\eta\tau} + f_\eta^2 - f f_{\eta\eta} + M^2 f_\eta = f_{\eta\eta} + k_1(S f_{\eta\eta\eta\tau} + 2 f_\eta f_{\eta\eta\eta} - f_{\eta\eta}^2 - f_{\eta\eta\eta\eta}) \tag{10}$$

$$S\theta_\tau + 2 f_\eta \theta - f\theta_\eta - \frac{1}{\Pr}\theta_{\eta\eta} = Ec\, f_{\eta\eta}^2 + M^2 Ec\, f_\eta^2 \tag{11}$$

And the corresponding boundary conditions are transformed to,

$$\begin{aligned} &f_\eta(0, \tau) = \sin \tau, \quad f(0, \tau) = 0, \quad \theta(0, \tau) = 1 \\ &f_\eta(\infty, \tau) = 0, \quad f_{\eta\eta}(\infty, \tau) = 0, \quad \theta(\infty, \tau) = 0 \end{aligned} \tag{12}$$

Where $\Pr = \frac{\mu c_p}{K}$ is the prandtl number, $k_1 = \frac{k_0 b}{\nu}$ is the dimensionless viscoelastic parameter. Here $k_1 = 0$

corresponds to the case of a Newtonian fluid. $M^2 = \frac{\sigma B_0^2}{\rho b}$ is the Hartman number or the magnetic parameter, $Ec = \frac{b^2 l^2}{A c_p}$ is the Eckert number.

One of the physical quantities of interest, the local heat transfer rate in terms of Nusselt number can be expressed as:

$$Nu_x = \frac{x\, q_w}{K(T_w - T_\infty)} = -\mathrm{Re}_x^{1/2}\, \theta_\eta(0)$$

$$\text{where surface heat flux } q_w = -K\left(\frac{\partial T}{\partial y}\right)_{y=0} \tag{13}$$

$$i.e \quad Nu_x\, \mathrm{Re}_x^{-1/2} = -\theta_\eta(\eta,\tau) \quad at\ \eta = 0$$

Where $\mathrm{Re}_x = \frac{b\, x^2}{\nu}$ is the local Reynolds number.

For the solution of system of simultaneous differential equation as given in (10) and (11), with the conditions (12), the equations are reformulated as:

$$\begin{aligned} & f_\eta - h = 0 \\ & S\, h_\tau + h^2 - f\, h_\eta + M^2 h - h_\eta - k_1 (S\, h_{\eta\eta\tau} + \\ & 2h\, h\eta\eta - h_\eta^2 - h_{\eta\eta\eta}) = 0 \\ & S\theta_\tau + 2h\theta - f\theta_\eta - \frac{1}{\mathrm{Pr}}\theta_{\eta\eta} = Ec\, h_\eta^2 + M^2 Ec\, f\, h^2 \end{aligned} \tag{14}$$

And the corresponding boundary conditions now become:

$$\begin{aligned} & h(0,\tau) = \sin\tau, \quad f(0,\tau) = 0, \quad \theta(0,\tau) = 1 \\ & h(\infty,\tau) = 0, \quad h_\eta(\infty,\tau) = 0, \quad \theta(\infty,\tau) = 0 \end{aligned} \tag{15}$$

The system of simultaneous differential equations given in (14) along with the boundary conditions (15) is numerically solved using Element Free Galerkin Method (EFGM).

IV. Element free Galerkin method

The Element free Galerkin method (EFGM) requires **Moving least square (MLS)** interpolation functions to approximate an unknown function. The MLS approximant requires only set of nodes for its construction and is made up of three components: a compact support weight function associated with each node, a polynomial basis function and a set of coefficients that depends on node position. The weight function is non-zero over a small neighborhood at a particular node, called support domain of the node. Using MLS approximation, the unknown field variable u(x) is approximated over the domain Ω as (details can be seen in [14]):

$$u(x) \approx u^h(x) = \sum_{j=1}^{m} p_j(x) a_j(x) = p^T(x) a(x) \tag{16}$$

Where m is the number of terms in the basis, $p_j(x)$ the monomial basis function and $a_j(x)$ the non-constant coefficient functions. In the present simulation ***quadratic basis functions*** are used i.e. $p^T(x) = [1\ x\ x^2]$. The coefficients $a_j(x)$ are determined by minimizing the functional J(x) given by:

$$J(x) = \sum_{I=1}^{n} W(x - x_I) \left\{ \sum_{j=1}^{m} p_j(x_I) a_j(x) - u_I \right\}^2 \tag{17}$$

Where $W(x - x_I)$ is a weight function which is non-zero over a small domain, called support domain, n is the number of nodes is the support domain. The minimization of J(x) w.r.t a(x) leads to the following set of equations:

$$a(x) = A^{-1}(x) B(x) U_s \tag{18}$$

Where A and B are given as

$$\begin{aligned} & A(x) = \sum_{I=1}^{n} W(x - x_I) p(x_I) p^T(x_I) \\ & B(x) = \left[W(x - x_1) p(x_1), W(x - x_2) p(x_2), ..., W(x - x_n) p(x_n) \right] \\ & U_s = \left[u_1, u_2, ..., u_n \right] \end{aligned}$$

Substituting (18) in (16), the MLS approximant is obtained as:

$$u^h(x) = \sum_{I=1}^{n} \Phi_I(x) u_I = \Phi(x) u \tag{19}$$

Where the shape function $\Phi_I(x)$ is defined by:

$$\Phi_I(X) = \sum_{j=1}^{m} p_j(X) \left(A^{-1}(X) B(X) \right)_{jI} = p^T A^{-1} B_I \tag{20}$$

A. Weight Function Description

The weight function is non-zero over a small neighborhood of x_I, called the support domain of node I. The choice of weight function affects the resulting approximation $u^h(x_I)$ in EFG and other meshless methods. In EFGM, the continuity of MLS approximants is governed by the continuity of weight function. Singh et al. [15] has studied these weight functions and reported that cubicspline weight function gives more accurate results as compared to others. Therefore, in present work, cubicspline weight function has been used.

B. Cubic Spline Weight

$$W(r - r_I) = W(r) = \begin{cases} \frac{2}{3} - 4r^2 + 4r^3 & r \le 1/2 \\ \frac{4}{3} - 4r + 4r^2 - \frac{4}{3} r^3 & \frac{1}{2} < r \le 1 \\ 0 & r > 1 \end{cases}$$

$$\text{where } r_I = \frac{\| x - x_I \|}{d_{m_I}}, \quad d_{mx_I} = d_{\max} C_{x_I}$$

d_{mx_I} is the sizes of support domain in x-direction. $d_{\max}$ is a scaling parameter, and C_{x_I} is the distance to the nearest neighbor in x-direction. The size of the support domain at a particular node I is only controlled by scaling parameter since the distance between nearest neighbors for an evaluation point (or quadrature point) remains unchanged for a given nodal data distribution. The minimum value of $d_{\max}$ should be greater than 1 so that n>m, and the maximum value of $d_{\max}$ should be such that it preserves the local character of MLS approximation. The optimum range of scaling parameter for heat transfer problems is discussed in [16]. In the present simulation $d_{\max}$ has been fixed as 2.2.

C. Variational Formulation

The weighted integral form of the equations (14) over the entire domain can be written as:

$$\int_0^{\eta_{\max}} w_1\left(f_\eta - h\right) = 0$$

$$\int_0^{\eta_{\max}} w_2\left(\begin{array}{l} S\,h_\tau + h^2 - f\,h_\eta + M^2 h - h_\eta - k_1(S\,h_{\eta\eta\tau} + \\ 2hh\eta\eta - h_\eta^2 - h_{\eta\eta\eta}) \end{array}\right) = 0 \qquad (21)$$

$$\int_0^{\eta_{\max}} w_3\left(S\theta_\tau + 2h\theta - f\theta_\eta - \frac{1}{\Pr}\theta_{\eta\eta} - Ec\,h_\eta^2 - M^2 Ec\,f\,h^2\right) = 0$$

Where w_1, w_2, w_3 are arbitrary test functions and may be viewed as the variation in f, h, θ respectively.

D. Element Free Galerkin Formulation

The Element free Galerkin model of the equations (21) may be obtained by substituting MLS approximation for the unknown variables f, h, θ using equations (19-20).

$$f(\eta) = \sum_{I=1}^{n} \Phi_I(\eta) f_I(\tau), \quad h(\eta,\tau) = \sum_{I=1}^{n} \Phi_I(\eta) h_I(\tau),$$
$$\theta(\eta,\tau) = \sum_{I=1}^{n} \Phi_I(\eta)\theta_I(\tau) \qquad (22)$$

E. Imposition of the boundary conditions

Since MLS shape functions do not satisfy the kronecker delta property, so we cannot directly impose the essential boundary conditions. To remove this problem, different numerical techniques have been proposed to enforce the essential boundary conditions in EFG method, such as Lagrange Multiplier method, Penalty method. In the present simulation penalty method is applied.

F. Penalty Method

Using penalty method, to enforce the essential boundary conditions, the variational form is written as:

$$\int_0^{\eta_{\max}} w_1\left(f_\eta - h\right) + \bar{\alpha}\, w_1\left(f - f(0)\right)\big|_{\eta=0} = 0$$

$$\int_0^{\eta_{\max}} w_2\left(\begin{array}{l} S\,h_\tau + h^2 - f\,h_\eta + M^2 h - h_\eta - k_1(S\,h_{\eta\eta\tau} + \\ 2hh\eta\eta - h_\eta^2 - h_{\eta\eta\eta}) + \bar{\alpha}\left(h - h(0)\right)\big|_{\eta=0} \\ + \bar{\alpha}\left(h - h(\infty)\right)\big|_{\eta=\infty} \end{array}\right) = 0 \qquad (23)$$

$$\int_0^{\eta_{\max}} w_3\left(\begin{array}{l} S\theta_\tau + 2h\theta - f\theta_\eta - \frac{1}{\Pr}\theta_{\eta\eta} - Ec\,h_\eta^2 - M^2 Ec\,f\,h^2 \\ + \bar{\alpha}\left(\theta - \theta(0)\right)\big|_{\eta=0} + \bar{\alpha}\left(\theta - \theta(\infty)\right)\big|_{\eta=\infty} \end{array}\right) = 0$$

where $f(0),\ h(0),\ h(\infty),\ \theta(0),\ \theta(\infty)$ are given in equation (15). $\bar{\alpha}$ is the penalty parameter and in the present work, it is chosen as 10^6.

Using the EFGM model given by (22), into equations (23), the system of equations can be defined in matrix form, which is given as follows:

$$[K]\{\bar{H}\} + [M]\{\dot{\bar{H}}\} = \{F\} \qquad (24)$$

$$[K] = \begin{bmatrix} K_{11} & K_{12} & K_{13} \\ K_{21} & K_{22} & K_{23} \\ K_{31} & K_{32} & K_{33} \end{bmatrix}, [M] = \begin{bmatrix} 0 & 0 & 0 \\ 0 & M_2 & 0 \\ 0 & 0 & M_3 \end{bmatrix}$$

Where

$$\{\bar{H}\} = \begin{bmatrix} \{f\} \\ \{h\} \\ \{\theta\} \end{bmatrix}, \{\dot{\bar{H}}\} = \begin{bmatrix} \left\{\dot{f}\right\} \\ \left\{\dot{h}\right\} \\ \left\{\dot{\theta}\right\} \end{bmatrix}, [F] = \begin{bmatrix} \{F_1\} \\ \{F_2\} \\ \{F_3\} \end{bmatrix}$$

$$K_{11} = \int_0^{\eta_{\max}} \phi_I \frac{\partial \phi_J}{\partial \eta}\, d\eta + \bar{\alpha}\phi_I{}^T \phi_J\big|_{\eta=0},\ K_{12} = \int_0^{\eta_{\max}} -\phi_I^T \phi_J\, d\eta,\ K_{13} = 0$$

$$K_{21} = 0, K_{22} = \int_0^{\eta_{\max}} \left(\begin{array}{l} \bar{h}\,\phi_I\phi_J - \phi_I\,\bar{f}\,\frac{\partial \phi_J}{\partial \eta} + M^2\phi_I\phi_J\,\bar{h} + \frac{\partial \phi_I}{\partial \eta}\frac{\partial \phi_J}{\partial \eta} + \\ 2\,k_1\,\bar{h}\frac{\partial \phi_I}{\partial \eta}\frac{\partial \phi_J}{\partial \eta} + k_1\frac{\partial \bar{h}}{\partial \eta}\phi_I\frac{\partial \phi_J}{\partial \eta} - k_1\,\bar{f}\frac{\partial \phi_I}{\partial \eta}\frac{\partial^2 \phi_J}{\partial \eta} \end{array}\right) d\eta$$
$$+ \bar{\alpha}\phi_I{}^T\phi_J\big|_{\eta=0} + \bar{\alpha}\phi_I^T\phi_J\big|_{\eta=\infty}$$

$$K_{23}=0,\ K_{31}=0,\ K_{32}=\int_0^{\eta_{\max}}\left(-Ec\,\phi_I\frac{\partial\phi_J}{\partial\eta}\frac{\partial\bar{h}}{\partial\eta}-EcM^2\phi_I\phi_J\bar{h}\right)d\eta$$

$$K_{33}=\int_0^{\eta_{\max}}\left(-\phi_I\frac{\partial\phi_J}{\partial\eta}\bar{f}+\frac{1}{\Pr}\frac{\partial\phi_I}{\partial\eta}\frac{\partial\phi_J}{\partial\eta}\right)d\eta+\bar{\alpha}\phi_I^T\phi_J\Big|_{\eta=0}+\bar{\alpha}\phi_I^T\phi_J\Big|_{\eta=\infty}$$

$$(M_2)_{IJ}=\int_0^{\eta_{\max}}\left(S\,\phi_I\phi_J+k_1S\frac{\partial\phi_I}{\partial\eta}\frac{\partial\phi_J}{\partial\eta}\right)d\eta,M_3=\int_0^{\eta_{\max}}\left(S\,\phi_I^T\phi_J\right)d\eta$$

$$(F_1)_I=\bar{\alpha}f(0)\phi_I\Big|_{\eta=0},(F_2)_I=\bar{\alpha}h(0)\phi_I\Big|_{\eta=0}+\bar{\alpha}\,h(\infty)\phi_I\Big|_{\eta=\infty},$$

$$(F_3)_I=\bar{\alpha}\theta(0)\phi_I\Big|_{\eta=0}+\bar{\alpha}\,\theta(\infty)\phi_I\Big|_{\eta=\infty},$$

$$\bar{f}=\sum_{I=1}^{n}\Phi_I\bar{f}_I,\quad \bar{h}=\sum_{I=1}^{n}\Phi_I\bar{h}_I,\quad \bar{\theta}=\sum_{I=1}^{n}\Phi_I\bar{\theta}_I$$

For time integration, ***Crank-Nicolson scheme*** is used which is unconditionally stable. Following Crank-Nicolson scheme, eq. (24) at (p+1)th time step can be written as:

$$\left[\hat{K}\right]_{p+1}\left[\bar{H}\right]_{p+1}=\left[\hat{K}\right]_{p}\left[\bar{H}\right]_{p}+[F]_{p,p+1}$$

$$\text{where}\quad \left[\hat{K}\right]_{p+1}=[M]+\frac{\Delta t}{2}[K]_{p+1},\left[\hat{K}\right]_{p}=[M]-\frac{\Delta t}{2}[K]_{p}$$

$$[F]_{p,p+1}=\frac{\Delta t}{2}\left[\{F\}_p+\{F\}_{p+1}\right]$$

The whole domain Ω is discretized with uniformly distributed 101 nodes. Four point Gauss quadrature formula has been used to calculate the integral values. At each node three functions f,h,θ are to be evaluated, hence after assembly, we obtain a non-linear system of equations of order 303×303, as given in (24). Owing to the nonlinearity of the system an iterative scheme has been used to solve it with an initial guess. The system of equations is linearized by incorporating known functions $\bar{f},\bar{h},\bar{\theta}$, which is solved using Gauss elimination method. This gives a new set of values of unknowns f,h,θ and the process continues till the absolute difference of two successive iterate value of unknowns is less than the accuracy 0.0005.

It has been observed that in the same domain, the accuracy is not affected even if the numbers of nodes are increased, else it increases the computational time only.

V. Results And Discussion

In order to obtain some physical insight into present simulation, numerical computations are carried out for various values of the parameters that describe the flow characteristics and the results are reported in terms of graphs.

Fig. 2 shows the time series of the velocity field $h(=f_\eta)$ at the four different distances from the surface of the oscillatory sheet with fixed values of $S=1, M=2, \Pr=5.0, k_1=0.2, Ec=0.2$. It is observed that the amplitude of the flow near the oscillatory surface is greater as compared to that far away from the surface. As the distance increases from the surface, the amplitude of the flow motion is decreased and almost vanishes (approached to zero) for larger distance from the sheet.

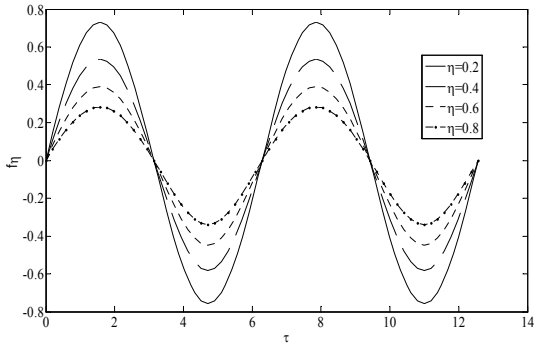

Fig. 2 $f_\eta(\eta,\tau)$ with S=1.0, M=2.0, k_1=0.4, Pr=5.0 and Ec=0.2

Fig. 3 depicts the effect of viscoelastic parameter k_1 on the time series $\tau\in[0,4\pi]$ of the velocity field $h(=f_\eta)$ at a fixed distance $\eta=0.2$ from the surface. An increment in the amplitude of the flow motion is observed with the increase of the non-Newtonain viscoelastic parameter k_1 due to increased effective viscosity.

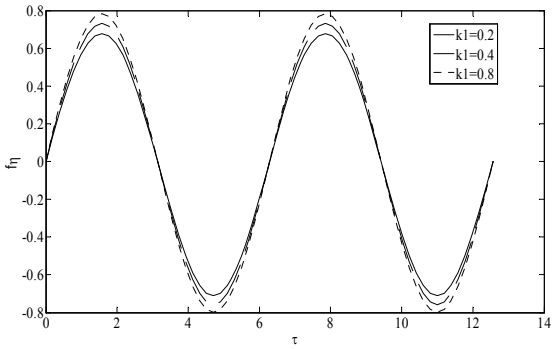

Fig. 3 $f_\eta(\eta,\tau)$ with S=1.0, M=2.0, Pr=5.0 and Ec=0.2

In Fig. 4 the effect of parameter S (ratio of oscillation frequency of sheet to its stretching rate) on the time series $\tau\in[0,4\pi]$ of the velocity field is depicted. It is observed that with the increase of *S* the amplitude of the flow increases slightly.

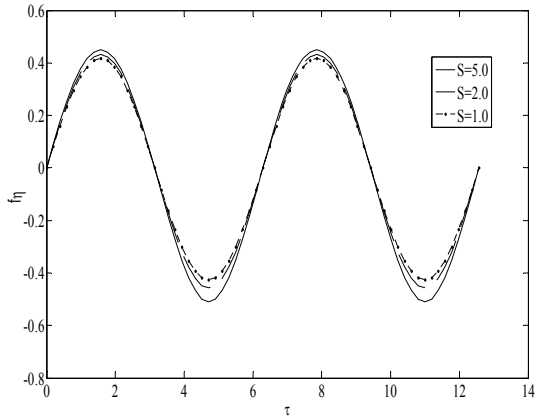

Fig. 4 $f_\eta(\eta,\tau)$ with k_1=0.2, M=2.0, Pr=5.0 and Ec=0.2, $\eta = 0.4$

Fig. 5 depicts the velocity profile f_η for the different values of the magnetic parameter M keeping fixed values of $S = 1.0,\ k_1 = 0.2, \Pr = 5.0, Ec = 0.2$. As expected, the magnetic field in an electrically conducting flow acts as a drag-like force called the Lorentz force. This type of resistive force tends to slow down the motion of the fluid in the boundary layer i.e decelerates the flow. Hence, the amplitude of the flow decreases with the increase of the magnetic parameter M. Due to deceleration of the flow, temperature of the fluid is increased. Fig. 6 reveals the relative influence of magnetic field on temperature $\theta(\eta,\tau)$.

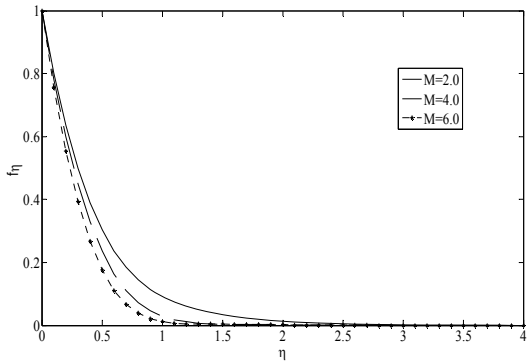

Fig. 5 $f_\eta(\eta,\tau)$ with k_1=0.2, S=1.0, Pr=5.0, Ec=0.2, $\tau = \pi/2$

Fig. 7 illustrates the effect of prandtl number Pr on the temperature profile $\theta(\eta,\tau)$ at $\tau = \pi/4$. It is observed that the effect of increasing Prandtl number Pr is to decrease, temperature throughout the boundary layer, which results in decrease of the thermal boundary layer thickness. The increase of Prandtl number means slow rate of thermal diffusion.

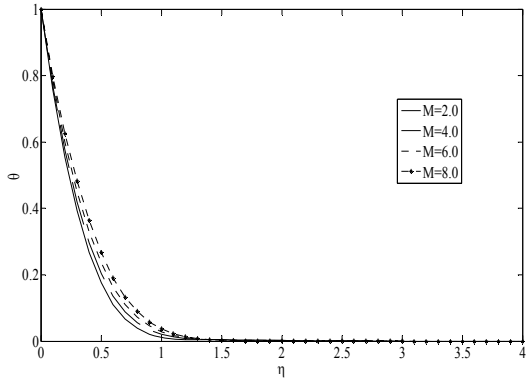

Fig. 6 $\theta(\eta,\tau)$ with k_1=0.2, S=1.0, Pr=5.0, Ec=0.2, $\tau = \pi/2$

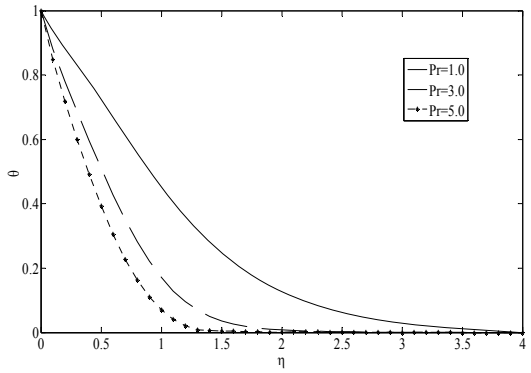

Fig. 7 $\theta(\eta,\tau)$ with k_1=0.2, S=1.0, M=2.0, Ec=0.2, $\tau = \pi/4$

Fig. 8 depicts that the effect of increasing the values of local Eckert number Ec is to increase temperature distribution in the flow region. This behavior of temperature enhancement occurs as heat energy is stored in the fluid due to frictional heating.

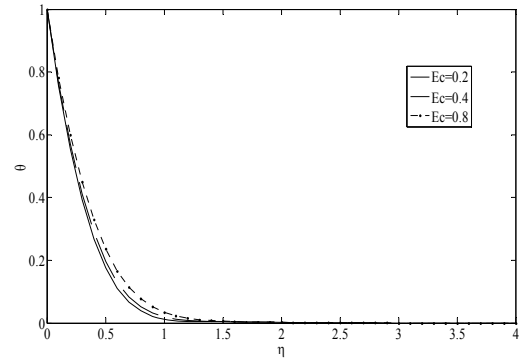

Fig. 8 $\theta(\eta,\tau)$ with k_1=0.2, S=1.0, Pr=5.0, M=2.0, $\tau = \pi/2$

VI. Conclusions

The main findings can be summarized as:

1. The effect of viscoelastic parameter is to increase the velocity distribution.

2. The effect of magnetic parameter is to decrease the velocity distribution while temperature increases with the increased magnetic parameter.
3. The thermal boundary layer thickness decreases significantly with the increase of Prandtl Number.
4. The effect of increasing values of Eckert number is to increase the temperature in the boundary layer flow.

TABLE I

COMPARISON OF RESULTS FOR THE NUSSELT NUMBER $-\theta_\eta(0)$ WITH k_1=0.0, M=0.0, S=0.0, Ec =0.0 AND VARIOUS VALUES OF Pr WITH CHEN [11] AND GRUBKA AND BOBBA [12]

Pr	Chen [11]	Grubka and Bobba [12]	Present Results
1.0	1.33334	1.3333	1.3333
2.0	-	-	1.9876
3.0	2.50972	2.5097	2.5095
5.0	-	-	3.6577
10.0	4.79686	4.7969	4.7968

ACKNOWLEDGMENT

One of the authors (Sonam Singh) would like to thank Council of Scientific and Industrial Research (CSIR), Government of India, for its financial support through the award of a research grant.

REFERENCES

[1] J.E. Dunn, K.R. Rajagopal, "Fluids of differential type – critical review and thermodynamic analysis", *Int. J. Eng. Sci.*, vol. 33 (1995) 689–729.
[2] B. C. Sakiadis, "Boundary-layer behavior on continuous solid surfaces: I. Boundary-layer equations for two-dimensional and axisymmetric flow", *AIChE Journal*, vol. 7 (1961) 26-28.
[3] L.J Crane, "Flow past a stretching plate", *J. App. Math. And Phys*., vol. 21 (1970) 645-647.
[4] C.Y. Wang, "Nonlinear streaming due to the oscillatory stretching of a sheet in a viscous fluid", *Acta Mech*., vol. 72 (1988) 261--268.
[5] V. Ambethkar, "A numerical study of heat and mass transfer effects on an oscillatory flow of a viscoelastic fluid with thermal relaxation", *Adv. Theor. Appl. Mech.*, vol. 3 (2010) 397-407.
[6] V.M. Soundalgekar, S.K. Gupta, "Free convection effects on the oscillatory flow of a viscous, incompressible fluid past a steadily moving vertical plate with constant suction", *Int. J. Heat Mass Transfer*, vol. 18 (1975) 1083--1093.
[7] Z. Abbas, Y. Wang, T. Hayat, M. Oberlack, " Hydromagnetic flow in a viscoelastic fluid due to the oscillatory stretching surface", *Int. J. Non-Linear Mech.*, vol. 43 (2008) 783-793.
[8] R. Sharma , R. Bhargava and P. Bhargava , "A numerical solution of unsteady MHD convection heat and mass transfer past a semi-infinite vertical porous moving plate using element free galerkin method", *Comput. Mater. Sci.*,vol. 48 (2010) 537-543.
[9] T. Belytscho , L. Gu , Y.Y. Lu , "Fracture and crack growth by element free Galerkin method", *Model. Simulat. Mater. Sci. and Engg.*, vol. 2 (1994) 519-534.
[10] S. Singh, R. Bhargava, " Element free Galerkin simulation of micropolar squeeze film flow of a biological lubricant", *J. Info. And Oper. Management*, vol. 3, (2012) 149-152.
[11] C. H. Chen, "Laminar mixed convection adjacent to vertical continuously stretching sheets", *Int. J. Heat Mass Transfer*, vol. 33 (1998) 471–476.
[12] L.T. Grubka and K.M. Bobba, "Heat transfer characteristic of a continuous stretching surface with variable temperature", *ASME J. heat transfer*, vol. 107 (1985b) 248-250.
[13] R.L. Fosdick K.R. Rajagopal, "Thermodynamics and stability of fluids of third grade", *Proc R Soc A,* vol. 369 (1980) 351–377.
[14] G.R. Liu, "Mesh free method-Moving beyond the Finite element method", CRC Press,2003, Ch. 5-6.
[15] A. Singh, I.V. Singh, R. Prakash, "Numerical analysis of fluid squeezed between two parallel plates by meshless method", *Comp. & fluids*, vol. 36 (2007) 1460-1480.
[16] I.V. Singh, "A numerical solution of composite heat transfer problems using meshless method", *Int. J. Heat Mass transfer*, vol. 47 (2004) 2123–2138.